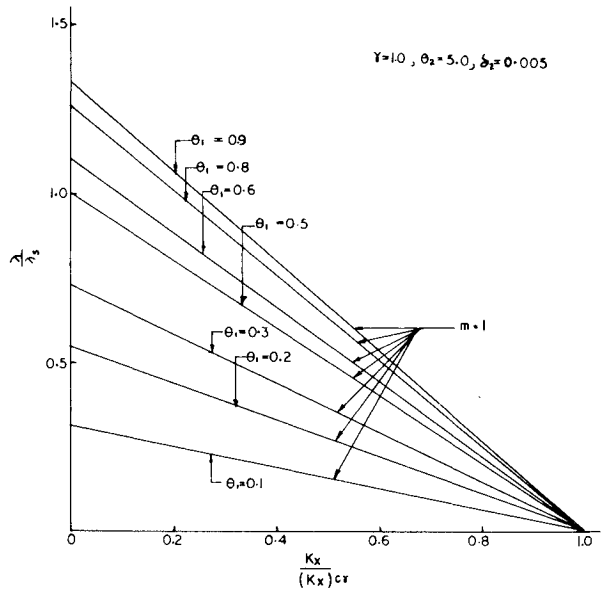

Fig. 5 Variation of frequency ratio with axial load ratio.

$\alpha_1 = 1.0$, $\psi_1 = 1.0$, $\nu_3 = 0.3$, $\gamma_1 = 1.0$, $\gamma_2 = 0.5$, $\beta = 0.0125$

The value of λ_s, the magnitude of which is 0.268×10^{-6}, corresponds to the frequency of an unsymmetrical square sandwich plate with $\theta_1 = 0.5$, $\theta_2 = 5.0$, and $\delta_2 = 0.005$, in addition to the preceding values of parameters. $(K_x)_{cr}$ is the nondimensional critical load of the plate under consideration. The other parameters listed in Figs. 2–5 are chosen so as to clearly point out the effect of axial load on the frequencies and on the modal pattern of the sandwich plate.

The influence of uniaxial compression on the frequencies can be observed in all cases as shown in Figs. 2–5. The frequencies are greatly reduced with the increase in axial loads and finally become zero at those corresponding to the buckling loads of the plates. It is also observed that the vibrational modes vary in the vicinity of the buckling load. From Fig. 2, it is seen that the modal patterns are affected when the aspect ratio γ is greater than 1. At $\gamma = 4$, the value of m is found to be as high as 8 just prior to buckling, unlike the case of homogeneous plates.[5] This sort of behavior can mainly be attributed to the shear deformation of the core.[6] For the case of a square plate with a weak core, it can be seen from Fig. 3 that the lowest frequencies correspond to $m = 2$ in the vicinity of the buckling load. Similar observation can also be made for a square plate having sufficiently thick core, as shown in Fig. 4. However, it is to be pointed out that the asymmetry of the faces has no influence on the modal number m for a particular sandwich plate. This can be seen from Fig. 5.

Conclusions

Free vibration analysis of unsymmetrical sandwich plates under uniaxial compression has been presented in this Note. It is shown that the frequencies and vibrational modes are greatly influenced depending upon the material and geometrical properties of the plate. This effect is found to be more predominant when the axial load approaches the critical value.

References

[1] Habip, L. M., "A Survey of Modern Developments in the Analysis of Sandwich Structures," *Applied Mechanics Reviews*, Vol. 18, No. 2, Feb. 1965, pp. 93–98.

[2] Hoff, N. J., "Bending and Buckling of Rectangular Sandwich Plates," TN 2225, 1950, NACA.

[3] Rao, Y. V. K. S. and Nakra, B. C., "Vibratory Bending of Unsymmetric Sandwich Plates," *Archives of Mechanics*, Vol. 25, No. 2, 1973, pp. 213–225.

[4] Shahin, R. M., "Free Vibrations of Multilayer Sandwich Plates in the Presence of Inplane Loads," *The Journal of Astronautical Sciences*, Vol. XIX, No. 36, May–June, 1972, pp. 433–447.

[5] Herrmann, G., "The Influence of Initial Stress on the Dynamic Behavior of Elastic and Viscoelastic Plates," *Publications of the International Association for Bridge and Structural Engineering*, Vol. 16, 1956, pp. 275–294.

[6] Plantema, F. J., *Sandwich Construction*, Wiley, New York, 1966.

Evaluation of a Wedge Gas-Sampling Probe

H. Lee Beach Jr.*
NASA Langley Research Center, Hampton, Va.

Introduction

Gas sample profiles transverse to the main flow direction can be obtained quite successfully in many high temperature mixing and reacting flowfields with water-cooled, multiple probe rakes similar to that described in Ref. 1. The size and spacing of the probes in such a rake are determined not only by the physical dimensions of the flowfield, but also by the cooling required and consideration of interference effects between the probes. In small-scale flowfields, the combination of these constraints can make fabrication extremely costly if feasible at all. For example, scaling the probe rake described in Ref. 1 (probe diameter = 0.65 cm, spacing = 1.9 cm) for use in a flow 2.5 cm wide would require unrealistically small probe diameters of 0.11 cm with a spacing of 0.3 cm. A composition profile can be obtained, of course, by stepping a single probe of the Ref. 1 type transverse to the flow; however, this approach is not feasible for many applications due to test duration limitations.

Two alternative techniques suitable for small-scale flows are discussed in Ref. 2. One is a blunt leading edge wedge probe with multiple stagnation ports on the leading edge; the other is a sharp leading edge wedge probe with static sampling ports on the wedge surface. The attractive features of these probes are the potential for locating sampling ports very close together and the relatively simple fabrication and cooling. Substantially different results were obtained with the stagnation and static wedge probes in the supersonic mixing/reacting flow described in Ref. 2. Temperature and pressure rises associated with the detached bow shock ahead of the blunt leading edge of the stagnation probe were found to significantly alter the reaction kinetics relative to those of the static probe which had its sampling surface aligned with the flow. Another potential problem with the blunt-edged probe exists even when kinetics are not important. If the flow approaching the shock is nonuniform (in Mach number, concentration, flow direction), the relative streamline orientations behind the shock may be different from those ahead of the shock. Samples entering the stagnation ports will therefore misrepresent the undisturbed spacing of the flow in line with the ports. This is not expected to be a problem with the wedge-static probe.

To determine the acceptability of a probe similar to the static-sampling wedge probe of Ref. 2 in a small-scale flow (region of interest, 1.9 cm) pertinent to supersonic combustion ramjet research, a wedge probe has been designed, fabricated

Received January 18, 1974; revision received March 13, 1974.
Index categories: Airbreathing Propulsion, Hypersonic; Combustion in Gases.

* Aerospace Technologist, Combustion Section, Hypersonic Vehicles Division.

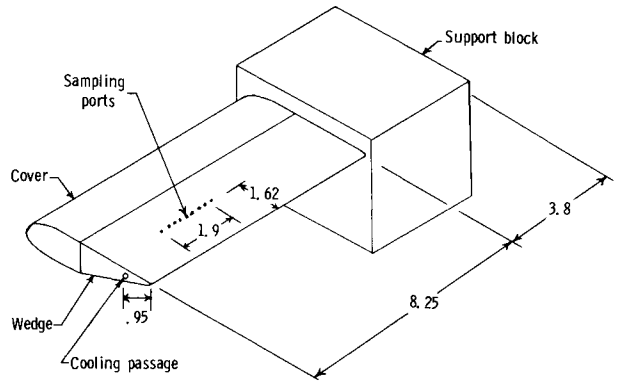

Fig. 1 Schematic of wedge gas-sampling probe (dimensions are in centimeters).

and evaluated by comparing its results with those obtained with a reliable pitot/sampling probe. The flowfield chosen for establishing this comparison was a hydrogen-vitiated air diffusion flame.

Apparatus and Procedure

A schematic of the wedge sampling probe is shown in Fig. 1. It is constructed of copper, and consists of a support block, a 20° included angle wedge, and a cover to protect the instrumentation tubes. Cooling is provided by water supplied internally to the cover and to a passage drilled parallel to the leading edge. The wedge sampling surface is mounted at 2° to the main flow direction and has nine sample ports 0.5 mm in diameter and 2.4 mm apart. The wedge leading edge has a radius of 0.38 mm to reduce stagnation point heat transfer rates.

A description of the pitot sampling probe used to obtain comparative data is given in detail in Ref. 1. Important features are a conical probe tip with 20° half-angle, and a 0.79-mm-diam orifice. The experimental apparatus providing reacting flow for these tests is described in Ref. 3. It consists of an axisymmetric, Mach 2, 6.53-cm-diam test gas nozzle supplying vitiated air, and a Mach 2, 9.5 mm injector supplying coflowing hydrogen mounted on the centerline of the larger nozzle. Test gas is provided by a hydrogen-oxygen air burner which is fueled in proportions such that the resulting combustion products have a volume fraction of oxygen equal to that of air, a nominal total temperature of 2220 K, and a total pressure of 0.689 MN/m^2.

Results for the tests consisted of gas sample measurements transverse to the main flow direction at an axial location approximately 20 cm downstream of the hydrogen injection; at this location both axial and radial concentration gradients were significant, and comparison of data from the two probes was expected to provide a good test of the wedge technique. Both wedge and pitot probe samples were collected in 75 cm^3 cylinders by evacuating the cylinders, purging them with sample gases, and filling them to an appropriate pressure level. Total sampling time for a set of 9 samples from the wedge probe was approximately 8 sec. Pitot samples were obtained one at a time and required approximately 6 sec each, excluding the time required to step the probe to a new radial location; significantly more time was thus required to obtain the same number of samples with the pitot probe. The time problem of pitot sampling was highly amplified by test duration limitations which allowed only one sample acquisition per burner firing. Time and propellent savings by use of the wedge probe were therefore much greater than sampling time alone indicates. Samples were

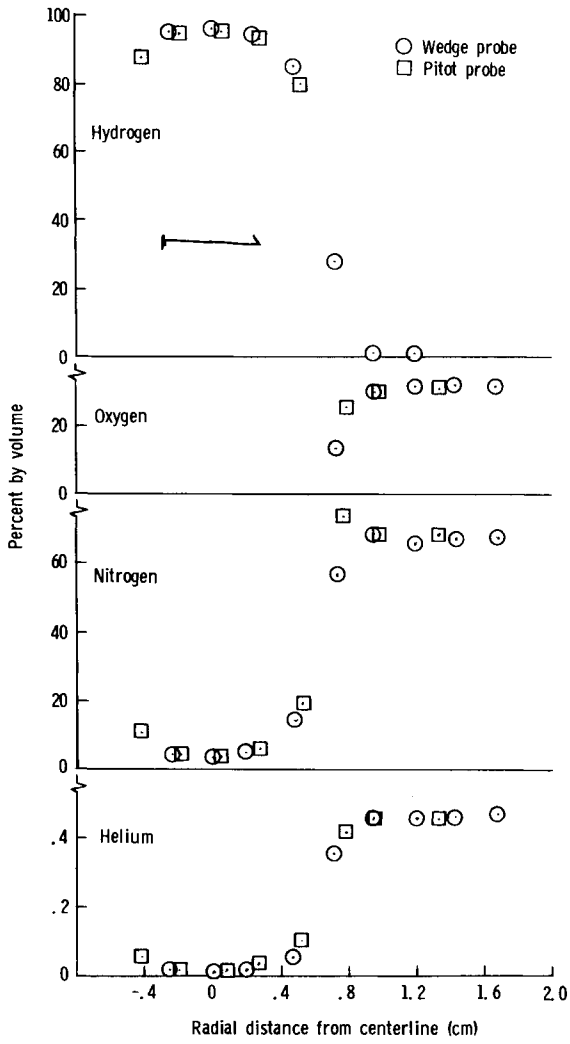

Fig. 2 Dry composition profiles.

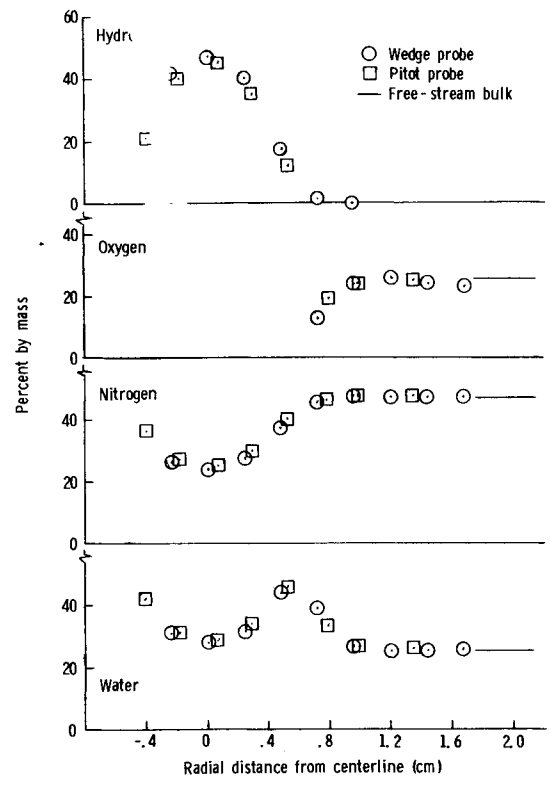

Fig. 3 Wet composition profiles.

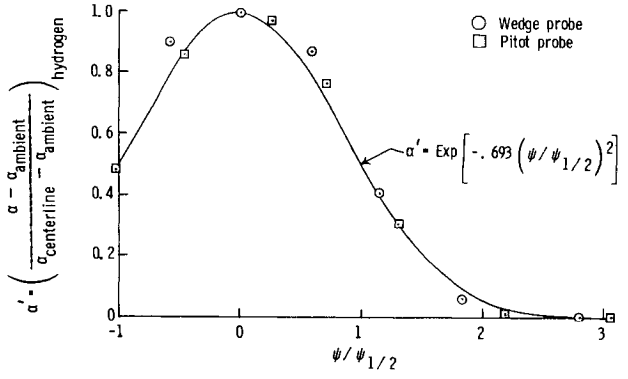

Fig. 4 Normalized hydrogen composition profiles.

analyzed by a gas chromatograph; since the collection cylinders were not heated, water in the samples condensed and results were obtained in the form of dry volume fractions of nitrogen, oxygen, and helium. Helium was used to trace the oxygen supplied to the burner.

Results and Discussion

Radial profiles of dry sample volume fractions as analyzed by the gas chromatograph are given for both probes in Fig. 2. Note that approximately the same radial distance was covered with each probe, but no attempt was made to match sample locations exactly. Results are given for both sides of the flow centerline to show symmetry, and extend through the mixing/reacting zone into the freestream. For all constituents the agreement between wedge and pitot results is quite good. Note also that the wedge sample at a radial distance of 0.72 cm contains both unreacted hydrogen and oxygen; this is probably due to unmixedness as described by several sources including Ref. 4.

To account for the water present in the samples, a data reduction computer program incorporating a mass balance and measured flow rates to the test gas supply was utilized. Plots of the resulting "wet" analysis which represents local stream composition are given in Fig. 3 in the form of calculated mass fractions of hydrogen, oxygen, nitrogen and water. Here, as in Fig. 2, the agreement between wedge probe and pitot probe data is good. The results appear reasonable in the sense that the region of depleted hydrogen and oxygen in Figs. 2 and 3 correspond as anticipated to a peak in the water profile, and the freestream values correspond closely to the bulk values computed from measured propellant flows to the burner.

A further validity check can be made by plotting the data in similarity-type form. According to Ref. 5, a concentration profile representable by a Gaussian distribution should be expected. Figure 4 shows such a plot, where the normalized concentration α' is the difference between local and freestream hydrogen concentrations divided by the difference in centerline to freestream values, and these concentrations have been converted to the unreacted state. The abscissa is the Von Mises coordinate ψ normalized by $\psi_{\frac{1}{2}}$, the value of ψ where α' is 0.5. The ψ values for the data points are computed by the technique described in Ref. 4; they are used in lieu of radial coordinates to eliminate the effect of heat release on the results. Both wedge and pitot data agree well with the Gaussian distribution, and are concluded to be reasonable.

Conclusions

Composition data obtained with the wedge and pitot probes agree well in regions with and without strong gradients. This implies that neither chemical nor boundary-layer effects induced by use of the wedge probe are different from those of the pitot probe. The wedge probe shows good survival qualities, produces results which appear to be valid, and allows total sampling time to be greatly reduced; it is therefore judged to be an accurate and useful data acquisition tool for small-scale, supersonic reacting flowfields.

References

[1] Rogers, R. C. and Eggers, J. M., "Supersonic Combustion of Hydrogen Injected Perpendicular to a Ducted Vitiated Airstream," AIAA Paper 73-1322, Las Vegas, Nev., 1973.

[2] Lengelle, G. and Verdier, C., "Gas Sampling and Analysis in Combustion Phenomena," AGARD-AG-168, July 1973, pp. 49–53.

[3] Beach, H. L., Jr., "Supersonic Mixing and Combustion of a Hydrogen Jet in a Coaxial High Temperature Test Gas," AIAA Paper 72-1179, New Orleans, La., 1972.

[4] Anderson, G. Y., Agnone, A. M., and Russin, W. R., "Composition Distribution and Equivalent Body Shape for a Reacting, Coaxial, Supersonic Hydrogen-Air Flow," TN D-6123, Jan. 1971, NASA.

[5] Zakkay, V., Krause, E., and Woo, S. D. L., "Turbulent Transport Properties for Axisymmetric Heterogeneous Mixing," *AIAA Journal*, Vol. 2, No. 11, Nov. 1964, pp. 1939–1947.

Basic Limitation in Microwave Measurement of Plasma Temperature

A. SINGER* AND J. M. MINKOWSKI†
The Johns Hopkins University, Baltimore, Md.
Harry Diamond Laboratories, Washington, D.C.

THE electron temperature of shock-heated plasma can be determined, in principle, from microwave measurements. In all such determinations reported heretofore,[1-3] the electron temperature t_e is computed from three other measured or estimated plasma parameters—the radiation temperature t_r, and the power reflection and transmission coefficients, R and T, respectively—from the equation

$$t_r = (1-R-T)t_e = (1-R)(1-e^{-\alpha l})t_e \qquad (1)$$

where α is the absorption per unit distance and l is the thickness of the plasma. [When T is negligible but a diffraction component is present, a modified form of Eq. (1) is used.[4]]

A major assumption implicit in Eq. (1) is a step rise in temperature at the plasma boundary. This assumption is usually not valid because the shock-heated plasma produced in the laboratory is enveloped in a thin thermal boundary layer that sustains the temperature difference between the plasma and the surrounding medium. It is the purpose of this Note to examine the effect of this boundary layer on microwave measurements of electron plasma temperature.

Power Flow

The available microwave noise power from a blackbody at a uniform temperature t can be approximated by ktB, where k is Boltzmann's constant and B is the bandwidth under consideration. (The error in this approximation is about $2.5f_0/t\%$,[5] where f_0 is the center rf of the system in gigahertz, and t is in Kelvin.) For a partially transparent (gray) body, the available microwave noise power may be approximated[6] by $ktB(1-e^{-\alpha l})$.

Received January 25, 1974. Discussions with G. Bekefi of MIT, F. M. Davidson of The Johns Hopkins University, and M. Apstein of the Harry Diamond Laboratories were very helpful, and are gratefully acknowledged. We would also like to thank W. E. Phillips of the National Bureau of Standards for reviewing the manuscript.

Index categories: Plasma Dynamics and MHD; Shock Waves and Detonations.

* Research Engineer, Harry Diamond Laboratories; also Research Associate, Department of Electrical Engineering.

† Associate Professor, Department of Electrical Engineering.